FEMS Microbiology Ecology, 97, 2021, fiab004

doi: 10.1093/femsec/fiab004
Advance Access Publication Date: 11 January 2021
Research Article

RESEARCH ARTICLE

Dechloromonas and close relatives prevail during hydrogenotrophic denitrification in stimulated microcosms with oxic aquifer material

Clara Duffner[1,2,†], Sebastian Holzapfel[3], Anja Wunderlich[3], Florian Einsiedl[3], Michael Schloter[1,2] and Stefanie Schulz[2,*]

[1]Chair of Soil Science, TUM School of Life Sciences Weihenstephan, Technical University Munich, Emil-Ramann-Straße 2, 85354 Freising, Germany, [2]Research Unit Comparative Microbiome Analysis, Helmholtz Zentrum München, Ingolstädter Landstr. 1, 85764 Neuherberg, Germany and [3]Chair of Hydrogeology, Technical University Munich, Arcisstraße 21, 80333 Munich, Germany

*Corresponding author: Research Unit Comparative Microbiome Analysis, Helmholtz Zentrum München, Ingolstädter Landstr. 1, 85764 Neuherberg, Germany. Tel: +49 89 3187 3054; E-mail: stefanie.schulz@helmholtz-muenchen.de

One sentence summary: Members of the bacterial family *Rhodocyclaceae*, especially *Dechloromonas*, were detected as the major denitrifiers under hydrogenotrophic conditions in a groundwater-sediment microcosm experiment.

Editor: Lee Kerkhof

†Clara Duffner, http://orcid.org/0000-0001-7517-8434

ABSTRACT

Globally occurring nitrate pollution in groundwater is harming the environment and human health. *In situ* hydrogen addition to stimulate denitrification has been proposed as a remediation strategy. However, observed nitrite accumulation and incomplete denitrification are severe drawbacks that possibly stem from the specific microbial community composition. We set up a microcosm experiment comprising sediment and groundwater from a nitrate polluted oxic oligotrophic aquifer. After the microcosms were sparged with hydrogen gas, samples were taken regularly within 122 h for nitrate and nitrite measurements, community composition analysis via 16S rRNA gene amplicon sequencing and gene and transcript quantification via qPCR of reductase genes essential for complete denitrification. The highest nitrate reduction rates and greatest increase in bacterial abundance coincided with a 15.3-fold increase in relative abundance of *Rhodocyclaceae*, specifically six ASVs that are closely related to the genus *Dechloromonas*. The denitrification reductase genes *napA*, *nirS* and clade I *nosZ* also increased significantly over the observation period. We conclude that taxa of the genus *Dechloromonas* are the prevailing hydrogenotrophic denitrifiers in this nitrate polluted aquifer and the ability of hydrogenotrophic denitrification under the given conditions is species-specific.

Keywords: nitrate pollution; remediation; *Rhodocyclaceae*; groundwater; hydrogen oxidation; denitrification genes

INTRODUCTION

Nitrate leaching into groundwater as a result of intensified nitrogen fertilization and animal farming has been a severe global environmental problem since the 1970s (Rivett *et al.* 2008). Monitoring of the nitrate levels in the upper aquifers in Germany (EEA monitoring network) showed that 18% of groundwater wells had nitrate concentrations above 0.8 mM (50 mg NO_3/L) (Keppner, Grimm and Fischer 2017) and are thereby classified as polluted according to the European nitrate directive

Received: 6 May 2020; **Accepted:** 8 January 2021

(91/676/EEC, 1991). In the aquatic environment and the gastrointestinal tract bacteria reduce nitrate to nitrite. The later binds to haemoglobin at its active site thus impairing the oxygen-binding capacity, which can be fatal for infants (Greer and Shannon 2005). Additionally, epidemiological studies reported significant correlations between increased occurrence of colorectal cancer and the consumption of nitrate-enriched drinking water, even at concentrations far below 0.8 mM (Schullehner *et al.* 2018; Ward *et al.* 2018). Thus, minimizing nitrate concentrations in groundwater, widely used as the main source of drinking water, is important to ensure human health in the long run.

Denitrification is the dominant nitrate transformation process in groundwater and thus a natural biotic process of nitrate remediation (Rivett *et al.* 2008). It is defined as an energy gaining dissimilatory transformation of nitrate or nitrite to a gas species (Zumft 1997). However, under aerobic conditions, the denitrification capacity is poor and microbial available electron donors such as dissolved organic carbon (DOC) or reduced sulphur are often limited in groundwater (Wild, Mayer and Einsiedl 2018). Thus, the *in situ* addition of an electron donor into groundwater, potentially stimulating oxygen consumption and subsequently denitrification, represents a powerful remediation strategy for nitrate polluted aquifers (Janda *et al.* 1988; Smith *et al.* 2001; Chaplin *et al.* 2009). Hydrogen was proven to be the most practical electron donor for this purpose because autotrophic hydrogenotrophic denitrification leads to less bioclogging as it only reaches 40% of the cell yield compared to heterotrophic denitrification (Ergas and Reuss 2001). Additionally, no by-products requiring post-treatment may be formed (Karanasios *et al.* 2010). Also it is likely that aquifers naturally harbor hydrogenotrophic chemolithoautotrophic bacteria because a large proportion of the bacterial population in aquifers holds the genetic potential to fix CO_2 via the Calvin cycle (Herrmann *et al.* 2015) and hydrogenase genes occur over a wide range of phyla and environments (Greening *et al.* 2015). Microcosm experiments with sediment stemming from nitrate polluted oxic aquifers and hydrogen addition showed complete nitrate removal but with transient nitrite accumulation (Schnobrich *et al.* 2007; Chaplin *et al.* 2009). However, to the best of our knowledge the only *in situ* experiment conducted so far reported incomplete nitrate reduction and no reduction of nitrite (Chaplin *et al.* 2009). While some denitrifiers perform four steps reducing nitrate to gaseous N_2, others may only perform a subset due to lack of genes or unfavorable environmental conditions (Graf, Jones and Hallin 2014; Lycus *et al.* 2017). Since the denitrification intermediate nitrite is toxic and nitrous oxide represents an potent greenhouse gas (Mosier 1998), it is important to understand which hydrogenotrophic denitrifiers perform complete denitrification.

Confirmed autotrophic hydrogenotrophic denitrifiers in pure cultures belong to the genera *Acidovorax*, *Paracoccus*, *Acinetobacter* and *Pseudomonas* (Szekeres *et al.* 2002; Vasiliadou *et al.* 2006b). Additionally, *Rhodocyclus*, *Sulfuricurvum*, *Hydrogenophaga* and *Dechloromonas* were detected by 16S rRNA gene sequencing of stable communities in hydrogen-based bioreactors (Zhang *et al.* 2009; Zhao *et al.* 2011). *Hydrogenophaga* and *Dechloromonas* as well as *Sulfuritalea* were also detected as dominant transcriptionally active hydrogenotrophic denitrifiers in a microcosm experiment with groundwater and crushed rock from a pristine aquifer (Kumar *et al.* 2018a). These results from hydrogen-based bioreactors and pristine groundwater enrichments indicate which bacterial taxa are capable of autotrophic hydrogenotrophic denitrification. However, it is unknown which taxa would dominate upon hydrogen addition in a nitrate polluted oxic porous aquifer where *in situ* remediation seems to be an effective tool to reduce nitrate below drinking-water maximum allowable concentrations of 0.8 mM. Therefore, a microcosm experiment with sediment and groundwater from a tertiary aquifer located in southeast Germany was conducted under a hydrogen atmosphere measuring microbial nitrate reduction over time. The sampling area is characterized by intensive pig farming with groundwater nitrate concentrations up to 1.61 mM, high median oxygen concentrations of up to around 200 μM and, median DOC of only 11.8 μM (Wild, Mayer and Einsiedl 2018). Based on modelling results, the same authors determined a denitrification lag time (time prior to commencement of denitrification) of approximately 114 years for this aquifer, which illustrates the need for bioremediation in addition to reducing nitrogen input into groundwater. Over the course of the experiment microcosms were sampled destructively at several timepoints to determine the microbial community composition with 16S rRNA gene amplicon sequencing. We hypothesized that if the community changes upon hydrogen addition, the relative abundance of the hydrogenotrophic denitrifying community should increase as nitrate concentrations decrease. Additionally, denitrification genes and transcripts were quantified via (RT)-qPCR. Due to the highly selective conditions the diversity of denitrifiers in such aquatic environments is generally low (Zhang *et al.* 2009; Karanasios *et al.* 2010) and therefore an increased abundance of reductase genes and their corresponding transcripts may reflect the hydrogenotrophic denitrifiers of this community. The goal was to determine the predominant members of hydrogenotrophic denitrifier communities and which genes involved in denitrification were most abundant in the stimulated microcosms with oxic aquifer material.

METHODS

Study site and sampling method

The Hohenthann area is located 90 km northeast of Munich (Germany) within the Bavarian Tertiary Molasse-Hills. Both a main porous aquifer and several perched aquifers are nitrate polluted, electron donor limited and oxic. Sediment samples were taken from the main porous aquifer, whereas groundwater was collected from a spring discharging from one of the small perched aquifers. More details concerning the physicochemical parameters of the area and the oxygen reduction rates can be found in Wild, Mayer and Einsiedl (2018). Sampling for this study was done in August 2018. The sediment samples were taken on a fallow field (GPS: 48°42′01.2″N 12°00′10.2″E) with an auger from the saturated zone of the aquifer at a depth between 2 and 2.5 m. The groundwater discharging from the spring has on average 100 μM DOC. The sediment and groundwater were transported to the laboratory at <10°C and stored at 4°C prior to the experiment.

Microcosm experiment set up and sampling

Prior to the experiment the collected wet sediment was sieved (2 mm) to remove larger gravel and the groundwater was filtered (pore size ~20 μm) to remove particles. A total of 30 g of sieved sediment and 85 mL groundwater were added to 120 mL vials closed with butyl rubber septa and aluminium crimp caps. Overall, 69 vials were prepared. A total of four vials were sampled at the start of the experiment (0 h), simultaneous to the treatment's application, to assess the initial community. A total of forty vials were sparged with approximately 1 L of hydrogen (H_2) using a hydrogen generator (Precision series, Peak Scientific, Scotland).

Another eight vials were sparged with nitrogen as an anaerobic control lacking an electron donor (N_2), while eight vials with ambient air served as an untreated control (UC) and nine vials autoclaved prior to hydrogen sparging served as an abiotic control (sterile). At each sampling point four vials were destructively sampled so that the remaining microcosms stayed undisturbed. The sampling timepoints, and applied analyses of each treatment and control are stated in Table 1. Some sampling timepoints of the hydrogen-treated samples were excluded from the microbial analysis because the results of the chemical analysis did not suggest changes in the microbial community composition. The sterile controls were also excluded from the microbial analysis since DNA sequencing cannot differentiate between living and dead bacteria. The absence of oxygen in the hydrogen- and the nitrogen-treated microcosms was confirmed in four vials with an oxygen sensor (Fibox 4 trace, PreSens, Germany). During the experiment, all microcosms were incubated at 16°C on a rotary shaker (220 rpm). For the microbiological analyses two times 15 mL mixed sediment-groundwater suspension were centrifuged for 10 min at 7700 × *g* and 4°C. The supernatant was discarded, the pellets shock-frozen in liquid nitrogen and stored at −80°C until further processing. The samples for the chemical analysis were filtered (0.22 μm PES) to remove bacteria and analysed via ion chromatography (DIONEX ICS-1100, Thermo Fisher Scientific, Waltham, MA, USA). Nitrate and nitrite were measured in all vials while ammonium was only measured in one replicate per timepoint. The concentration of each sample is the mean of three measurements and the detection limits are 0.008 mM for nitrate, 0.007 mM for nitrite and 0.013 mM for ammonium.

Nucleic acid extraction and reverse transcription

DNA was extracted from one complete pellet (15 mL groundwater-sediment suspension) using the phenol–chloroform based protocol described in Lueders, Manefield and Friedrich (2004) and Töwe *et al.* (2011) and quantified fluorometrically. Due to the overall low DNA output, the RNA was extracted separately with the RNeasy Power Soil Total RNA Kit (QIAGEN, Hilden, Germany) from the second pellet sampled and quantified spectrophotometrically. Residual DNA in the extracts was digested with DNase (TURBO DNase, Thermo Fisher Scientific (Invitrogen), Waltham, MA, USA) with 1 μg RNA as input. The RNA was purified (RNA Clean & Concentrator-5 Kit, Zymo Research, Irvina, CA, USA) and the absence of DNA in the samples was confirmed using a *nirS* based qPCR according to the protocol in Table S3 (Supporting Information). Confirmation with a 16S rRNA gene-based PCR was not considered as useful due to known DNA contamination in laboratory reagents (Salter *et al.* 2014). Instead *nirS* was chosen as a marker gene because quantification on the DNA level (Fig. 5A) showed a high abundance of *nirS* genes in all samples. Furthermore, the RNA's quality was determined with a Fragment Analyzer (DNF-471 Standard Sensitivity RNA Analysis Kit, Agilent Technologies, Santa Clara, CA, USA). The extracted RNA of one hydrogen-treated vial from timepoint 30 h had a noticeable lower RNA quality number (RQN) of 3.5 compared to the rest of the samples (RQN 7.12, SD: 0.77). The sample with the low RQN value was omitted from further analysis, however three replicates of the timepoint remained. The purified RNA was quantified fluorometrically so that consistently 40 ng RNA were added to the reverse transcription reaction (High-Capacity cDNA Reverse Transcription Kit, Thermo Fisher Scientific (Applied Biosystems), Waltham, MA, USA). The two negative extraction controls and two DNase reaction controls were run alongside the samples.

16S rRNA gene amplicon sequencing, data processing and statistical analysis

Bacterial community composition was determined by 16S rRNA gene-targeted Illumina MiSeq amplicon sequencing. The hypervariable regions V1 and V2 of the 16S rRNA gene were amplified over 25 cycles with the adapter containing primer pair S-D-Bact-0008-a-S-16 5′-AGAGTTTGATCMTGGC-3′ and S-D-Bact-0343-a-A-15 5′-CTGCTGCCTYCCGTA-3′ (Klindworth *et al.* 2013) in triplicates. Besides the primers, the PCR reaction contained the NebNext High-Fidelity 2X PCR Master Mix (New England BioLabs, Ipswich, MA, USA) and 2 ng/μL DNA. Triplicates were pooled when the successful amplification was confirmed by an agarose gel and purified (AMPure XP Beads, Beckman Coulter, Brea, CA, USA). The amplicon's size, concentration and purity were determined by capillary electrophoresis. A total of 10 ng DNA were used as input in the following index PCR which added sample-specific indices (Nextera Dual Indexes Set, Illumina, San Diego, CA, USA) to the adapters during eight cycles. The indexed amplicons were also purified and analysed by capillary electrophoresis as described above. Afterwards they were equalized to 4 nM, pooled and loaded on the Illumina MiSeq platform with 20% PhiX for paired-end sequencing with the Reagent Kit v3 (2 × 300 bp; Illumina).

The demultiplexed sequenced reads were processed with QIIME 2 (Bolyen *et al.* 2019). Denoising was performed with the DADA2 plugin whereby the N-terminal trimming was set to 10 bp and the C-terminal trimming to 260 bp for the forward and to 220 bp for the reverse reads. The amplified sequence variants (ASVs) with reads in the negative extraction control were removed from all samples. For the taxonomic assignment (P-confidence ≥ 0.9), a classifier was pre-trained with the primer pair 0008/0343 based on the SILVA 16S database release 132 (Quast *et al.* 2012). To compensate for unequal sampling depth subsampling to the minimum number of reads per sample (17 515) was performed using the vegan package (version v2.4–2; Oksanen *et al.* 2019) in R project (version 3.5.3; R Development Core Team 2019). Data analysis was performed in R project using additional packages. The alpha diversity indices (Shannon and Simpson) were calculated with the vegan package (version v2.4-2; Oksanen *et al.* 2019) and converted to the effective number of species (ENS) by taking the exponent of the Shannon index and by dividing one by the complement of the Simpson index (Hill 1973). The stacked bar plots were generated with the phyloseq package (version 1.30.0; McMurdie and Holmes 2013) and the heatmap with the ComplexHeatmap package (Gu, Eils and Schlesner 2016). Because relative abundances are non-parametric data, a robust one-way ANOVA with trimmed means (t1way function) and the corresponding post-hoc test lincon, both from the package WRS2 (Mair and Wilcox 2019), were used to test which taxa differed in relative abundance over time. Low abundant taxa were removed from the tests when the sum of reads of a given taxa in all samples was less than four. Differences were considered significant if p-values were <0.05 after Benjamini–Hochberg correction (Benjamini and Hochberg 1995). The closest relatives of unclassified ASVs which increased significantly over time were determined with the nucleotide Basic Local Alignment Search Tool (nblast) by aligning the ASV sequence against the rRNA/ITS databases (NCBI: https://blast.ncbi.nlm.nih.gov/Blast.cgi). Because the percentage identity was

Table 1. Description of the microcosms experiment set up including the sampling time points, number of replicates and the performed subsequent analyses (x) for the treatments (H_2 and N_2) and controls (UC and sterile).

Treatment	None	H_2										N_2		UC		Sterile + H_2		
Time [h]	0	30	40	50	60	70	80	92	100	114	122	77	126	76	125	0	72	128
Replicates	4	4	4	4	4	4	4	4	4	4	4	4	4	4	4	3	3	3
Chemical analysis	x	x	x	x	x	x	x	x	x	x	x	x	x	x	x	x	x	x
Microbial analysis	x	x		x	x	x	x	x			x	x	x	x	x			

below 97%, additionally maximum-likelihood phylogenetic trees were created using MEGA-X (Kumar *et al.* 2018b). The phylogenetic trees were generated with the 324 bp long amplicon sequences and trimmed 16S rRNA gene sequences of closely related type species downloaded from the SILVA database (Quast *et al.* 2012). The amplicon sequence dataset is available in the Sequence Read Archive (SRA) repository under the BioSample accession numbers SAMN14610043-SAMN14610054 as part of the BioProject PRJNA626487.

Quantification of denitrification genes and transcripts

The genes and transcripts of all relevant reductases (Table S2, Supporting Information) were quantified by qPCR on a 7300 Real-Time PCR System (Applied Biosystems). Additionally, the overall bacterial abundance was determined by quantifying the 16S rRNA gene. To avoid PCR inhibition the optimal dilutions were determined for DNA (denitrification genes 1:25, 16S rRNA gene 1:500) and cDNA (1:8, only for clade II *nosZ* undiluted) by a dilution series qPCR. The standards were serially diluted ranging from 10^7 to 10^1 gene copies/μL. The standards of all genes, except for clade II *nosZ*, consisted of the respective gene fragment (source bacteria stated in Table S3, Supporting Information) inserted into a plasmid. The plasmid backbone however inhibited the clade II *nosZ* gene amplification. Therefore, clade II *nosZ* was amplified, purified and quantified to be used as a linear standard prior to starting the qPCR run. The qPCR reactions, performed in 96-well plates, contained Power Sybr Green Master Mix (Applied Biosystems), 0.2–1 μM forward and reverse primer (Table S3, Supporting Information) and 2 μL diluted DNA/cDNA. Additionally, the qPCR reactions of all genes, except for clade II *nosZ*, contained 0.06% BSA while the reactions of the clade II *nosZ* qPCRs contained 0.25 μg T4 Gene 32 protein. The qPCRs had an initial 10 min denaturation step at 95°C followed by gene-specific cycling conditions listed in Table S3 (Supporting Information). The specificity of the amplified products was verified by a melting curve analysis and agarose gels of exemplary samples. The R^2 of all standard curves was above 0.99 and the efficiencies, listed in Table S4 (Supporting Information), were calculated as described in Töwe *et al.* (2010) with the equation Eff $= 10^{(-1/\text{slope})} - 1$. The gene and transcript copy numbers were calculated per mL sediment-groundwater suspension. The differences in mean gene/transcript copy numbers were statistically tested with a robust ANOVA from the R package WRS2 (Mair and Wilcox 2019). As done for the analysis of sequencing data, tests with *P*-values <0.05 after Benjamini–Hochberg correction (Benjamini and Hochberg 1995) were considered significant.

RESULTS

Chemical analysis

The groundwater and sediment sampled from a highly nitrate polluted oxic oligotrophic aquifer inside sealed microcosms was sparged with hydrogen gas to stimulate the hydrogenotrophic denitrifying bacteria. Figure 1 shows the measured nitrate, nitrite and ammonium concentrations over time. In contrast to the nitrogen-treatment and the untreated control, the hydrogen-treatment stimulated denitrification up to complete nitrate and nitrite reduction. The initial nitrate concentration was fully reduced within 80 h. At the beginning, nitrate was reduced at an average rate of 6.6 μM/h however between 60 and 80 h the nitrate reduction rate increased to more than 35.6 μM/h. During this exponential phase of nitrate reduction, the nitrite concentrations peaked with the highest measured concentration (0.252 mM) after 70 h. Nitrite was still measured when nitrate was below detection limit but was also fully reduced after at least 92 h. A small amount of nitrate was also reduced in the nitrogen-treated and untreated control microcosms, however at much lower average rates (N_2: 2.68 μM/h, UC: 0.88 μM/h) (Fig. 1). The sterile control microcosms, however, displayed no nitrate reduction at all. Throughout the experiment ammonium concentrations remained below 0.024 mM in the measured vials.

Community analysis

The bacterial community composition in the groundwater and sediment suspensions was determined by 16S rRNA gene amplicon sequencing. On average the samples contained 113 283 sequence reads of which 54.2% were lost during denoising (Table S1, Supporting Information). The sampling depth was sufficient as the rarefaction curves reached a plateau at the cut-off of 17 515 reads (Fig. S1, Supporting Information). The effective number of species (ENS; Fig. 2A) decreased by half in the hydrogen-treated microcosms from an initial average ENS of 2099 to 915 within the first 30 h. The ENS in the nitrogen-treated and untreated control microcosms also decrease to around 1000, so this early drop can be attributed to the incubation rather than to the treatment. However, contrary to the controls the ENS in the hydrogen-treated microcosms further decreased between 30 and 80 h to average 235. The ENS based on the Simpson index (Fig. S2, Supporting Information) shows comparable results. Concurrent, 16S rRNA gene copies increased significantly over time ($P = 0.002$, t1way), especially between 60 and 92 h ($P = 0.009$, lincon; Fig. 2B), while no significant changes over time were observed in the nitrogen-treated microcosms and the untreated control.

The phylum *Bacteroidetes* increased significantly from 5.76% mean relative abundance at the beginning to above 10% after 60 h in the hydrogen-treated microcosms ($P = 0.001$, lincon; Fig. 3A and Fig. S4, Supporting Information). A similar increase in relative abundance also occurred in the nitrogen-treated (77 h, $P = 0.0009$ and lincon), and in the untreated control microcosms (76 h, $P = 0.0002$, lincon). Notably the mean relative abundance did not increase further thereafter in either treatments or control. The significant increase in *Bacteroidetes* was mainly attributed to the families *Crocinitomicaceae* and *Prolixibacteraceae* which both increased significantly in the hydrogen-treated ($P = 0.00003$, $P = 0.0004$, t1way) and nitrogen-treated microcosms (*P*

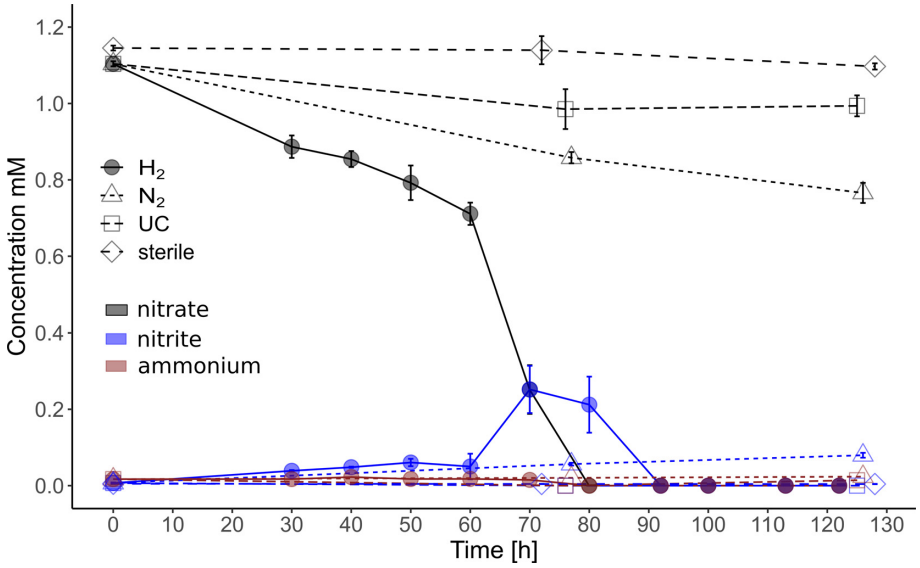

Figure 1. Nitrate, nitrite and ammonium concentrations over time in the hydrogen-treated (H_2), nitrogen-treated (N_2), untreated control (UC) and sterile microcosms. The data points for nitrate and nitrite are mean values from four replicates, except in the sterile control, where each data point is a mean value of three replicates. Error bars are SDs. The data points for ammonium are from one representative replicate.

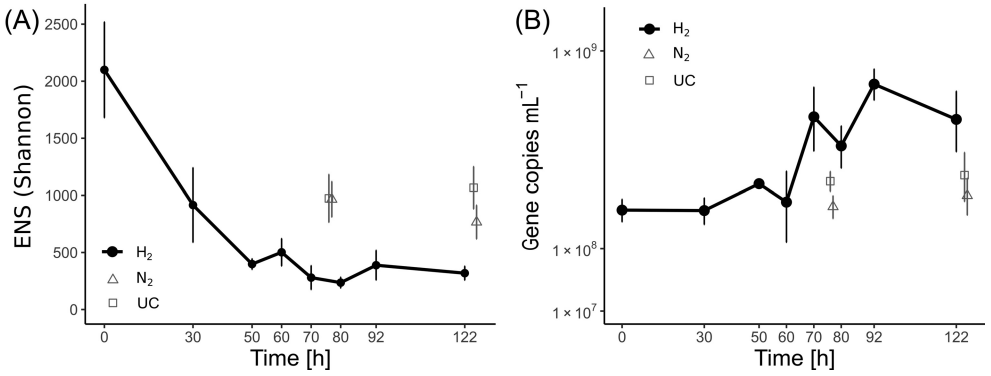

Figure 2. Changes in **(A)** the effective number of species (Shannon) based on the 16S rRNA gene amplicon sequencing data and **(B)** the bacterial abundance based on 16S rRNA gene quantification with qPCR in the hydrogen-treated, nitrogen-treated and untreated control microcosms over time. Timepoint 0 h represents the initial community independent from a treatment. The data points are mean values from four replicates; error bars are SDs.

= 0.047, P = 0.049, t1way; Fig. 3A). Also, in the untreated control, *Crocinitomicaceae* (P = 0.009, t1way) increased, however their relative abundance remained below 1.25% at all timepoints.

The second phylum which increased significantly over time was *Proteobacteria*. However, unlike *Bacteroidetes*, the increase was observed only in the hydrogen-treated microcosms (P = 0.00003, t1way; Fig. 3B and Fig. S4, Supporting Information). Its relative abundance rose from 37.9% at the beginning to 61.1% after 80 h, from then on it remained constant until the last measurement. A total of two families belonging to *Proteobacteria* contributed to the significant increase, namely *Rhodocyclaceae* (P = <0.00001, t1way) and *Burkholderiaceae* (P = 0.007, t1way). The former increased 15.3-fold in relative abundance from average 2 to 30.1% within the first 80 h while the later increased only 2.3-fold from average 5.8 to 13.5% within the same period. During the first 50 h, the relative abundance of *Rhodocyclaceae* increased at a rate of 0.1%/h which rose to 0.285%/h between 50 and 80 h, the period of the highest nitrate reduction rate and greatest increase in 16S rRNA copies. A first shift in the bacterial community composition of the hydrogen-treated microcosms between 30 and 50 h and a second shift after 60 h is visible in Fig. 3 and the heatmap (Fig. S3, Supporting Information), which includes the 40 most abundant ASVs of the phyla *Proteobacteria* and *Bacteroidetes* in the hydrogen-treated microcosms. In the hydrogen-treated microcosms, the significantly increased ASVs (t1way) of the first shift mostly belong to the family *Burkholderiaceae* e.g. *Rhodoferax*, as well as *Prolixibacteraceae* BSV13, *Fluviicola* and *Geobacter* (Fig. S3, Supporting Information). The genera *Curvibacter*, *Ramlibacter* and *Sulfuricella* also increased in relative abundance in the first 50 h however not statistically significant. Several ASVs which increased during the first community shift, including *Rhodoferax* and *Prolixibacteraceae*, also increased in relative abundance in the nitrogen-treated microcosms (Fig. S3, Supporting Information). However, these changes were not statistically significant. In contrast, the taxa belonging to the second shift, *Dechloromonas*, three unclassified *Rhodocyclaceae* ASVs (ii) and, two unclassified *Burkholderiaceae* ASVs (i), only enriched significantly in the hydrogen-treated microcosms but not in the nitrogen-treated nor in the untreated control (Fig. S3, Supporting Information). According to nblast and the created phylogenetic trees (Fig. S5, Supporting Information) the unclassified *Rhodocylcacea* ASVs (ii) are closely related to *Azospira*

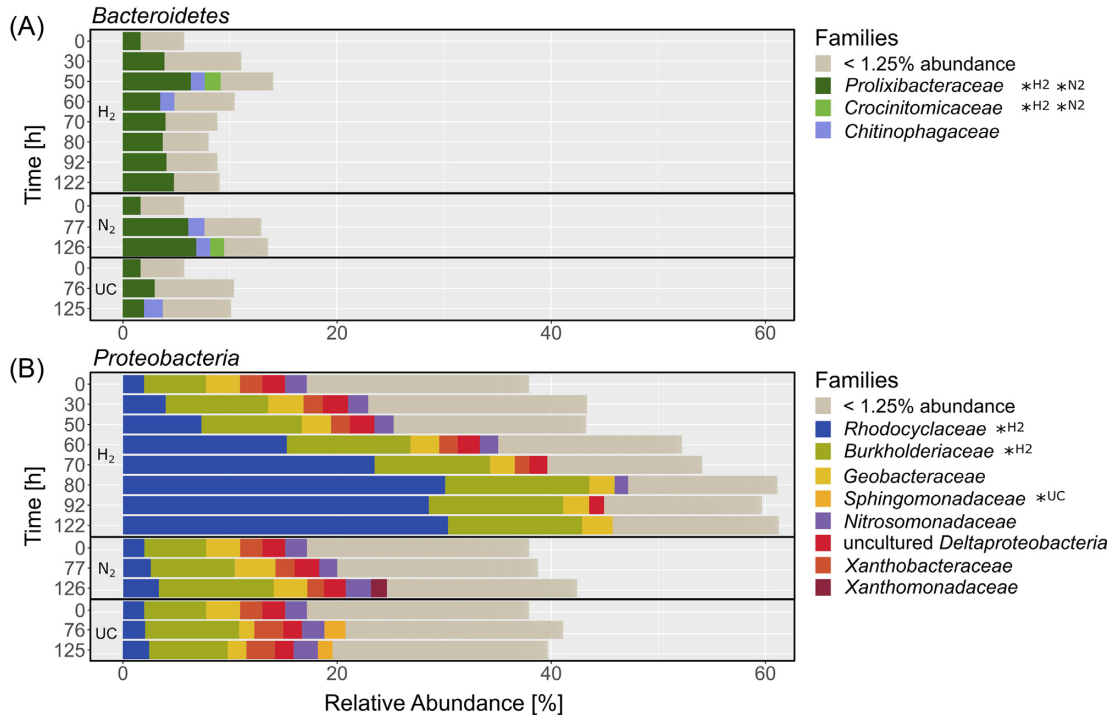

Figure 3. Changes in the bacterial community structure on the family level of the two phyla; **(A)** *Bacteroidetes* ($P = 0.00015$, t1way), and **(B)** *Proteobacteria* ($P = 0.00003$, t1way) which increased significantly in the hydrogen-treated microcosms over time. All significantly increased families (t1way) which reached at least 1.25% relative abundance at one timepoint are marked with an asterisk and the respective treatment/control it refers to (H_2: hydrogen, N_2: nitrogen, UC: untreated control). The stacked bars represent mean relative abundances of four replicates.

and *Rhodocyclus* and the unclassified *Burkholderiaceae* ASVs (i) are closely related to *Massilia*. *Sulfuritalea* increased in relative abundance within the first 50 h, like the taxa of the first community shift, and remained constant thereafter. The genus with the highest increase in relative abundance was *Dechloromonas* rising from on average 0.8% at the beginning to 24% after 80 h in the hydrogen-treated microcosms, while its relative abundance always remained below 1% in the nitrogen-treated microcosms and the untreated control (Fig. 4A). In the hydrogen-treated microcosms, 37 detected ASVs were assigned to the genus *Dechloromonas* of which only six increased significantly over time. Thereof, ASV15089, ASV5383 and ASV1396 were initially of such low abundance, that they remained below the detection limit even until 30 h. ASV15089 and ASV5383 increased in relative abundance until 92 h while ASV13899 and ASV9041 only increased until 70 to 80 h. A phylogenetic tree was constructed based on an alignment of the 324 bp long amplicon sequences of the 37 *Dechloromonas* ASVs and the trimmed 16S rRNA gene sequences of the type strains of all *Rhodocyclaceae* genera (Fig. 4B). It shows that the six *Dechloromonas* ASVs which increased significantly over time form three clusters within the *Dechloromonas* subtree. The monospecific genera *Ferribacterium* and *Quatrionicoccus* also position within the *Dechloromonas* subtree.

While the phyla *Bacteroidetes* and *Proteobacteria* increased significantly in relative abundance in the hydrogen-treated microcosms the phyla *Acidobacteria* ($P = 0.0003$, t1way), *Chloroflexi* ($P = 0.0005$, t1way), *Rokubacteria* ($P = 0.0005$, t1way) and *Nitrospirae* ($P = 0.02$, t1way) decreased significantly over time (Fig. S4, Supporting Information). No significant decrease in relative abundance of these phyla was observed in either the nitrogen-treated or the untreated control microcosms.

Denitrification genes and transcripts

In the hydrogen-treated microcosms the gene abundance of *napA* ($P = 0.001$, t1way), *nirS* ($P = <0.00001$, t1way), *qnorB* ($P = 0.045$, t1way) and clade I *nosZ* ($P = <0.00001$, t1way) increased significantly over time (Fig. 5A). Comparisons of all timepoints against each other using post-hoc test lincon showed significant differences between the timepoints 0–60 h and 70–122 h for the genes *napA*, *nirS* and clade I *nosZ* but not for *qnorB*. For *napA*, *nirS* and clade I *nosZ* the greatest increase was between 50 and 80 h while for *qnorB* only a slight gradual increase was measured. The mean gene abundance of *cnorB* also increased strongly between 60 and 92 h, however the variability between replicates was rather high. The copy number of most transcripts of the measured reductase genes increased from 60 to 80 h after which they decreased again (Fig. 5B). These changes were however mostly not significant. An exception were *nirK* transcripts, which did not increase at all, and clade I *nosZ* transcripts which started to increase in abundance earlier and peaked at 70 h. Significant changes in the abundance patterns of genes and transcripts of the analysed reductases over time were neither observed in the nitrogen treatment nor in the untreated control (Fig. 5).

DISCUSSION

In this study, we aimed to detect taxa stimulated under hydrogenotrophic denitrifying conditions, which were expected to increase in relative abundance during the period of greatest nitrate reduction activity. The maximum measured nitrate reduction rate of 35.6 μM/h, comparable with other studies on hydrogenotrophic denitrification (Ergas and Reuss 2001; Vasiliadou, Pavlou and Vayenas 2006a), was between 60 and 80 h. Con-

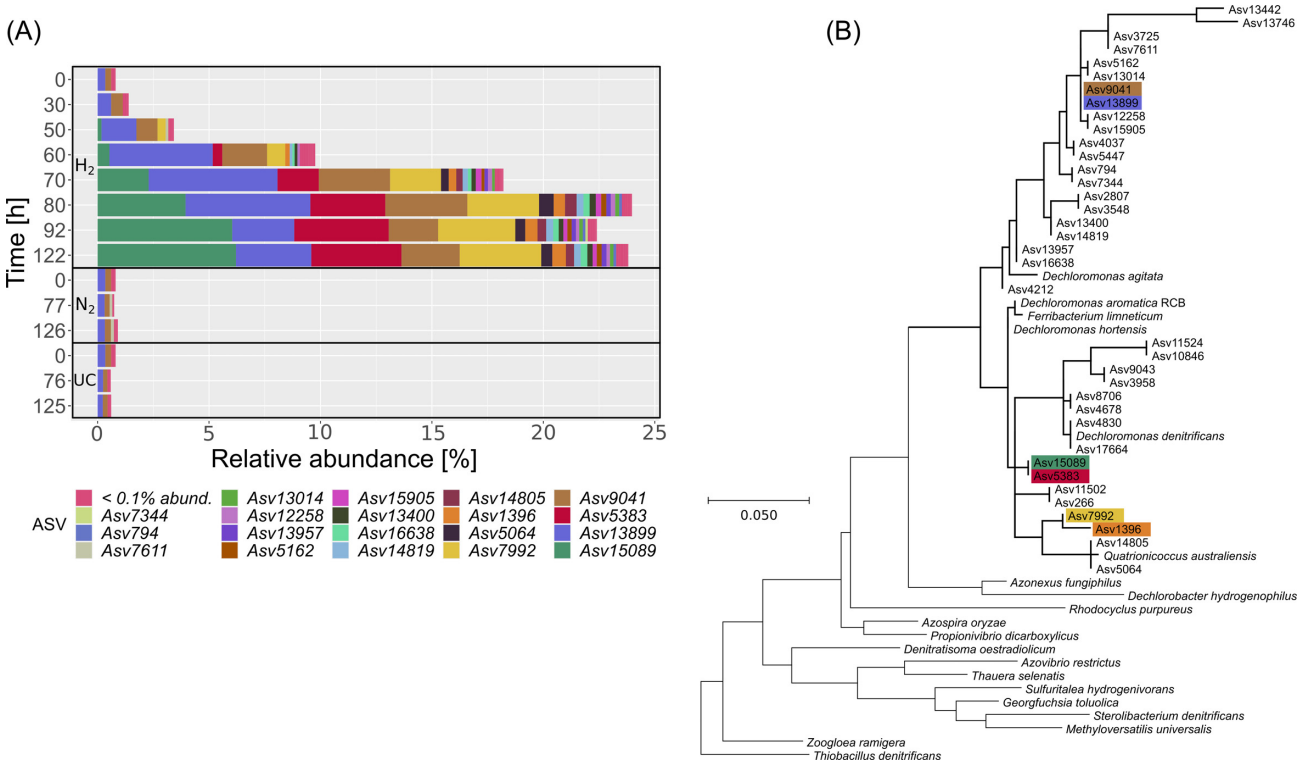

Figure 4. The stacked bar plot **(A)** shows the 37 detected ASVs assigned to the genus *Dechloromonas*. The stacked bars represent mean relative abundances of four replicates. Only six ASVs increased significantly in relative abundance in the hydrogen-treated microcosms. A phylogenetic tree **(B)** constructed with the amplicon sequences of the 37 detected *Dechloromonas* ASVs and 16S rRNA sequences of most type strains belonging to *Rhodocyclaceae*. The six ASVs which significantly increased over time (t1way) are marked with their respective color.

sequently, the highest energy gain and resulting greatest growth of bacteria utilizing hydrogen for denitrification is expected during this period. This is further corroborated by a decrease of ENS and a significant increase of 16S rRNA copies/mL between 60 and 92 h. The genera which increased greatest in relative abundance during this period were *Dechloromonas* and *Sulfuritalea* along with five unclassified ASVs which may belong to the genera *Azospira/Rhodocylcus* and *Massilia*. These taxa neither increased in the nitrogen-treated microcosms nor in the untreated control, which indicates that they were using hydrogen as the main electron donor. *Rhodocyclaceae*, the family with the greatest increase in relative abundance as it includes the genera *Dechloromonas*, *Azospira/Rhodocylcus*, *Sulfuritalea*, is known to contribute significantly to denitrification in wastewater treatment systems (Wang *et al.* 2020). The genera belonging to *Rhodocyclaceae* which increased significantly in relative abundance between 60 and 80h are all known hydrogenotrophic denitrifiers (Zhang *et al.* 2009; Zhao *et al.* 2011; Kumar *et al.* 2018a). Two unclassified ASVs likely belonging to the genus *Massilia* also increased in relative abundance between 60 and 80 h but contrary to the previous they belong to the family *Burkholderiaceae*. To our knowledge it has not been described as a hydrogenotrophic denitrifier yet whereby its role as such is questionable.

Dechloromonas was the genus with the greatest increase in relative abundance. Bacteria of this genus have been detected in many different environments and are known for their diverse abilities to degrade environmental contaminants such as aromatic hydrocarbons (BTEX; Bradford *et al.* 2018) and perchlorate (Salinero *et al.* 2009). They are also known to reduce nitrate, preferring it even over perchlorate, despite being energetically slightly less favorable (Nozawa-Inoue *et al.* 2011; Wang *et al.* 2018). Conthe *et al.* (2018) detected *Dechloromonas* as the most abundant clade II *nosZ* OTU in an enrichment culture grown on acetate and N_2O as the sole electron acceptor. This demonstrates the ability of *Dechloromonas* as a N_2O reducer. These qualities, which include wide occurrence, degradation of environmental contaminants as well as nitrate and strong N_2O reduction, are desirable traits in hydrogenotrophic denitrifiers for *in situ* remediation. The significant increase in relative abundance of only six out of 37 detected ASVs assigned to *Dechloromonas* implies species or even strain level differences in their hydrogenotrophic denitrifying abilitiy. This is further supported by differing behavior among these six *Dechloromonas* ASVs. While ASV13899 and ASV9041 increased in relative abundance only until 70–80 h, ASV15089 and ASV5383 continued, thereafter, when all nitrate had been reduced. Potentially ASV13899 and ASV9041 are incomplete denitrifiers, while ASV15089 and ASV5383 reduce all intermediates including nitrite, NO and N_2O as well. Generally, denitrification is a polyphyletic and ancient trait (Zumft 1997), so it is not unusual that even closely related taxa differ greatly in their denitrification characteristics (Liu *et al.* 2013) or in their genetic capability to denitrify (Jones *et al.* 2008; Graf, Jones and Hallin 2014). In the phylogenetic tree of *Rhodocyclaceae*, all 37 ASVs assigned to *Dechloromonas* clustered within the *Dechloromonas* subtree. The *Dechloromonas* subtree also includes the monospecific genera *Ferribacterium* and *Quatrionicoccus*, which can also be observed in other phylogenetic trees based on full 16S rRNA gene sequences (Oren 2014). Considering this, some ASVs which were assigned to the genus *Dechloromonas* by the used bioinformatic pipeline, could belong to the genera *Quatrionicoccus* or *Ferribacterium*. Of the six ASVs which seem to perform hydrogenotrophic

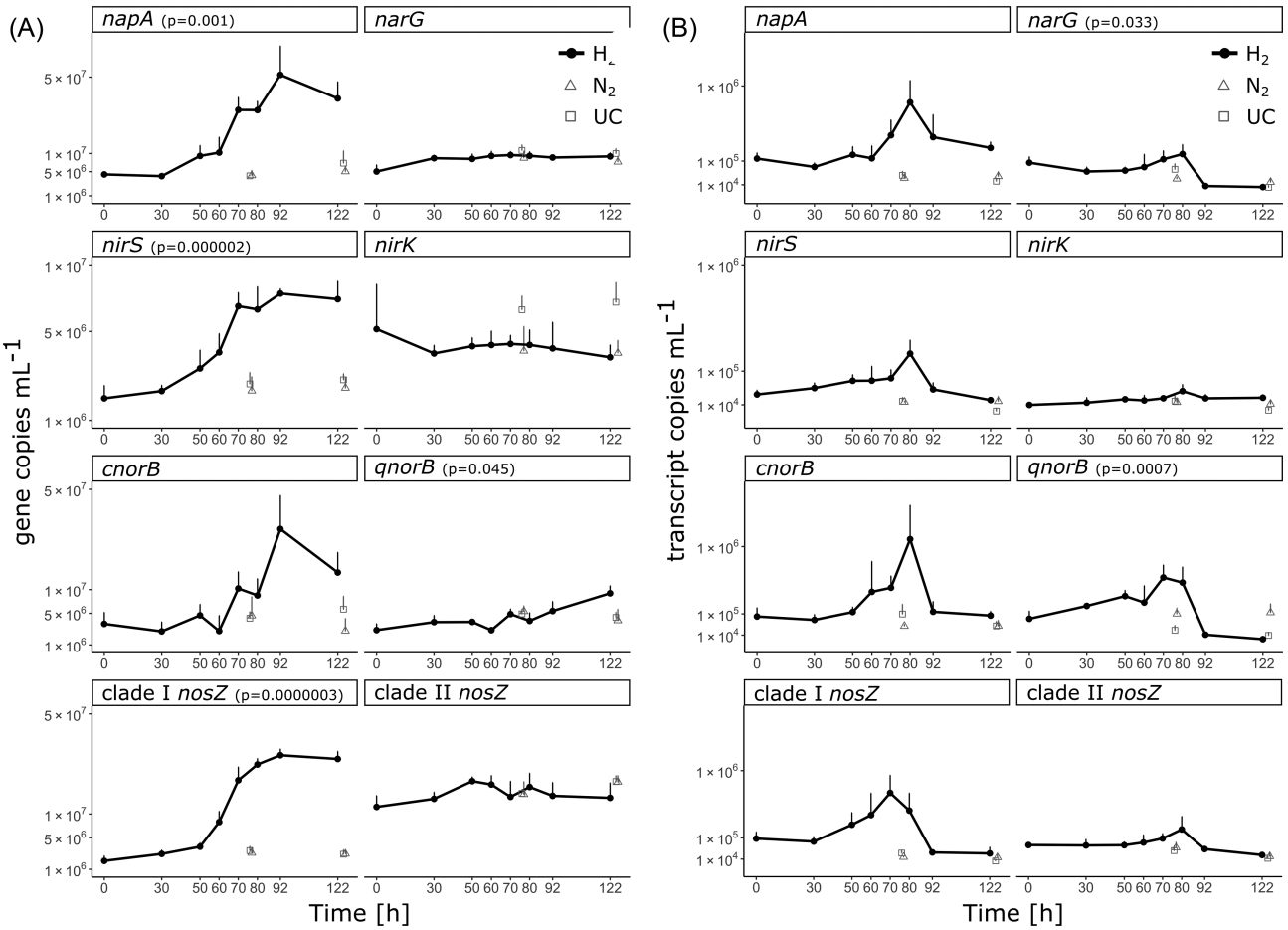

Figure 5. (A) Gene and **(B)** transcript abundance per mL sediment-groundwater suspension of the reductase genes *napA* and *narG* ($NO_3^- \rightarrow NO_2^-$), *nirS* and *nirK* ($NO_2^- \rightarrow NO$), *cnorB* and *qnorB* ($NO \rightarrow N_2O$), as well as clade I and clade II *nosZ* ($N_2O \rightarrow N_2$). The y-axes are square-root transformed, all data points are mean values of four replicates and error bars are SDs. Gene or transcript copy numbers differed significantly (t1way) only in the hydrogen-treated microcosms. The according *p*-values are stated. Timepoint 0 h represents the initial community independent from a treatment ($n = 4$).

denitrification, ASV7992 and ASV1396 clustered with *Quatrionicoccus australiensis* but none clustered with *Ferribacterium limneticum*. An identification beyond the genus level within the *Dechloromonas* subtree is however not feasible because the phylogenetic tree is only based on the 324 bp long amplicon sequences. These findings illustrate the need to isolate and analyse pure cultures of *Dechloromonas* and close relatives to elucidate the traits determining their hydrogenotrophic denitrification ability.

Clearly, the observed nitrate reduction in the hydrogen-treated microcosms was catalysed by microbiota because no nitrate reduction occurred in the sterile microcosms. Alternative metabolic pathways, such as dissimilatory nitrate reduction to ammonium (DNRA), are unlikely as denitrification may be favored over DNRA under carbon limitation and high nitrate availability in bacterial communities (Kraft *et al.* 2014). Also, throughout the experiment ammonium concentrations remained below 0.024 mM in all analysed microcosms. The increase in 16S rRNA gene copies in the hydrogen-treated microcosms, primarily between 60 and 92 h, confirms that the community composition changes resulted from an average 3.8-fold growth between 0 and 92 h rather than a partial decline due to death.

The gene copy numbers of *napA*, *nirS* and clade I *nosZ* increased significantly simultaneous from 50 h onwards. The amplicon sequencing results of the microcosm experiment confirmed the observation of other studies (Zhang *et al.* 2009; Karanasios *et al.* 2010) that hydrogenotrophic communities are stable and consist only of a few taxa. Consequently, *napA*, *nirS* and clade I *nosZ* are likely the pre-dominant denitrification reductases of the *Rhodocyclaceae* dominated community that increased in relative abundance in this study in parallel. Identification of the reductase genes in the genomes of three available *Dechloromonas* species (Table S5, Supporting Information) supports the obtained qPCR results of the nitrate and nitrite reductase, as all three analysed genomes contain one *napA* but no *narG* gene, and *nirS* but no *nirK* genes. While the nitric oxide reductase qPCR results were inconclusive, the qPCR results of *nosZ* indicate that clade I was the dominating nitrous oxide reductase. However, all three *Dechloromonas* genomes contain only clade II *nosZ* genes, thus we would have expected to see an increase in clade II *nosZ*, which was only the case on the transcript level. To check whether the observed increase in clade I *nosZ* can be attributed to another genus the available full genome sequences of *Azospira* and *Sulfuritalea* were also analysed (Table S5, Supporting Information), but either they contained clade II *nosZ* or no *nosZ* gene at all. Linking the qPCR results of the denitrification reductases to specific ASVs appears to be difficult as a direct proof of function and microbial identity is only possible with a metagenomics or amplicon sequencing

approach, which was beyond the scope of this study. Especially in the case of clade I and clade II *nosZ* the difference in the amplification products of the two qPCR makes a comparison difficult. The only published clade II *nosZ* qPCR amplifies a 690–720 bp long amplification product with a resulting low efficiency (Jones *et al.* 2013), while the clade I *nosZ* qPCR produces a 267 bp long amplification product (Henry *et al.* 2004). According to the RT-qPCR results, the expression of clade I *nosZ* began prior to the expression of the other reductases. Generally, the nitrate reductase is regulated separately and is expressed initially, while the other reductase genes share a common regulator in addition to individual ones (Bothe, Ferguson and Newton 2007). The temporal expression of the later differs between different species. When Bergaust *et al.* (2010) measured the gene expression in *Paracoccus denitrificans* every 2 h they found that the transcription of the *nosZ* gene started even some hours before the expression of *nirS* or *norB*. An early expression of *nosZ* gene is therefore not unlikely. However, a higher temporal resolution in the sampling timepoints would be required to detect a sequential expression.

The way each reductase type influences the phenotype is not fully understood. However, recent studies indicate advantageous attributes of *napA*, *nirS* and clade II *nosZ* type reductases, occurring in the detected dominant genera *Dechloromonas* and *Azospira*, for autotrophic hydrogenotrophic denitrifiers. For facultative bacteria switching from aerobic to anaerobic conditions and from organotrophy to lithotrophy a potential advantage of *napA* is its functional flexibility. Besides anaerobic respiration NapA can also perform redox-energy dissipation which is useful under sufficient carbon and oxygen conditions (Richardson *et al.* 2001). The multiple *nirS* gene copies detected in the *Dechloromonas* genomes (Table S5, Supporting Information; Wang *et al.* 2020), imply higher nitrite reduction rates due to increased transcription and subsequent protein production. An actual physiological advantage of clade II *nosZ* over clade I *nosZ* has been determined by Yoon *et al.* (2016). They could show that bacteria with known clade II *nosZ* had higher biomass yield and higher N_2O affinity compared to clade I *nosZ*. Additionally, clade II *nosZ* contains the signal peptide for Sec protein translocation into the periplasm while clade I *nosZ* contains the signal peptide for Tat protein translocation which requires substantially more energy (Lee, Tullman-Ercek and Georgiou 2006). The resulting higher metabolic efficiency of clade II NosZ reductases can be considered as a competitive advantage, especially in oligotrophic habitats.

The significantly increased taxa in the hydrogen-treated microcosms between 30 and 50 h, when the nitrate reduction rate was still low, receded once the second community shift emerged. These taxa, including *Rhodoferax* belonging to *Burkholderiaceae*, *Prolixibacteraceae* BSV13, *Fluviicola* and *Geobacter,* are not known as hydrogenotrophic denitrifiers. Some of these taxa increased in relative abundance, even though not significant, in the nitrogen-treated microcosms, which also displayed limited reduction of nitrate and steady increase in nitrite. Likely these taxa were growing on residual DOC from the sample material.

The initial bacterial community from the groundwater sediment suspension (0 h) was comparable to bacterial communities in similar upper section aquifers. For example, in an aquifer in France with high nitrate and oxygen concentrations in combination with low organic carbon (108 μM DOC; Ben Maamar *et al.* 2015) *Burkholderiaceae* was the dominating family and *Rhodocyclaceae* was also detected. *Burkholderiaceae* was also the family with the highest relative abundance at the beginning of this microcosm experiment. Notably, the taxa assigned to the family *Burkholderiaceae* in this study, according to the SILVA database release 132, were assigned to the families *Comamonadaceae* and *Oxalobacteraceae* in the study by Ben Maamar *et al.* (2015).

In conclusion, the present study revealed two community shifts. The first consisting of potential heterotrophic denitrifiers feeding on residual DOC and the second consisting of typical autotrophic hydrogenotrophic denitrifiers. Species of the genus *Dechloromonas*, and possibly also of their close relatives *Quatrionicoccus* and *Ferribacterium*, prevailed in the hydrogenotrophic denitrifier community and its members carry reductase genes, which likely favor facultative anaerobic lifestyle as well as high nitrite and N_2O reduction. The later suggests the genetic potential for complete denitrification which is additionally supported by the increased abundance of reductase genes involved in all four denitrification steps over time. The observed species- or even strain-level differences in the hydrogenotrophic denitrifying capabilities require isolation and analysis of isolates of the genera *Dechloromonas*, *Quatrionicoccus*, *Ferribacterium* as well as of close relatives from the family *Rhodocyclaceae* such as *Rhodocyclus* and *Azospira*.

ACKNOWLEDGMENT

We thank Susanne Thiemann from the Chair of Hydrogeology for the chemical analysis and Susanne Kublik from the Research Unit Comparative Microbiome Analysis for the MiSeq Illumina sequencing.

SUPPLEMENTARY DATA

Supplementary data are available at *FEMSEC* online.

FUNDING

Supported by Deutsche Forschungsgemeinschaft (DFG) through TUM International Graduate School of Science and Engineering (IGSSE), GSC 81.

Conflicts of Interest. None declared.

REFERENCES

Benjamini Y, Hochberg Y. Controlling the false discovery rate: a practical and powerful approach to multiple testing. *J R Stat Soc Ser B Methodol* 1995;**57**:289–300.

Ben Maamar S, Aquilina L, Quaiser A *et al.* Groundwater isolation governs chemistry and microbial community structure along hydrologic flowpaths. *Front Microbiol* 2015;**6**:1457.

Bergaust L, Mao Y, Bakken LR *et al.* Denitrification response patterns during the transition to anoxic respiration and post-transcriptional effects of suboptimal pH on nitrous oxide reductase in *Paracoccus denitrificans*. *Appl Environ Microbiol* 2010;**76**:6387–96.

Bolyen E, Rideout JR, Dillon MR *et al.* Reproducible, interactive, scalable and extensible microbiome data science using QIIME 2. *Nat Biotechnol* 2019;**37**:852–7.

Bothe H, Ferguson S, Newton W. *Biology of the Nitrogen Cycle*. Elsevier Science, 2007.

Bradford LM, Vestergaard G, Táncsics A *et al.* Transcriptome-stable isotope probing provides targeted functional and taxonomic insights into microaerobic pollutant-degrading aquifer microbiota. *Front Microbiol* 2018;**9**. DOI: 10.3389/fmicb.2018.02696.

Chaplin BP, Schnobrich MR, Widdowson M *et al*. Stimulating in situ hydrogenotrophic denitrification with membrane-delivered hydrogen under passive and pumped groundwater conditions. *J Environ Eng* 2009;**135**:666–76.

Conthe M, Wittorf L, Kuenen JG *et al*. Life on N2O: deciphering the ecophysiology of N2O respiring bacterial communities in a continuous culture. *ISME J* 2018;**12**:1142–53.

Ergas SJ, Reuss AF. Hydrogenotrophic denitrification of drinking water using a hollow fibre membrane bioreactor. *J Water Supply Res Technol Aqua* 2001;**50**:161–71.

Graf DRH, Jones CM, Hallin S. Intergenomic comparisons highlight modularity of the denitrification pathway and underpin the importance of community structure for N2O emissions. *PLoS One* 2014;**9**:1–20.

Greening C, Biswas A, Carere CR *et al*. Genomic and metagenomic surveys of hydrogenase distribution indicate H2 is a widely utilised energy source for microbial growth and survival. *ISME J* 2015;**10**:761.

Greer FR, Shannon M. Infant methemoglobinemia: the role of dietary nitrate in food and water. *Pediatrics* 2005;**116**:784–6.

Gu Z, Eils R, Schlesner M. Complex heatmaps reveal patterns and correlations in multidimensional genomic data. *Bioinformatics* 2016;**32**: 2847–9.

Henry S, Baudoin E, López-Gutiérrez JC *et al*. Quantification of denitrifying bacteria in soils by nirK gene targeted real-time PCR. *J Microbiol Methods* 2004;**59**:327–35.

Herrmann M, Rusznyák A, Akob DM *et al*. Large fractions of CO2-fixing microorganisms in pristine limestone aquifers appear to be involved in the oxidation of reduced sulfur and nitrogen compounds. *Appl Environ Microbiol* 2015;**81**:2384–94.

Hill MO. Diversity and evenness: a unifying notation and its consequences. *Ecology* 1973;**54**:427–32.

Janda V, Rudovský J, Wanner J *et al*. In situ denitrification of drinking water. *Water Sci Technol* 1988;**20**:215–9.

Jones CM, Graf DR, Bru D *et al*. The unaccounted yet abundant nitrous oxide-reducing microbial community: a potential nitrous oxide sink. *ISME J* 2013;**7**:417–26.

Jones CM, Stres B, Rosenquist M *et al*. Phylogenetic analysis of nitrite, nitric oxide, and nitrous oxide respiratory enzymes reveal a complex evolutionary history for denitrification. *Mol Biol Evol* 2008;**25**:1955–66.

Karanasios KA, Vasiliadou IA, Pavlou S *et al*. Hydrogenotrophic denitrification of potable water: a review. *J Hazard Mater* 2010;**180**:20–37.

Keppner L, Grimm F, Fischer D. *Nitratbericht 2016*, Bundesministerium für Umwelt, Naturschutz, Bau und Reaktorsicherheit (BMUB) & Bundesministeriumfür Ernährung und Landwirtschaft (BMEL), 2017.

Klindworth A, Pruesse E, Schweer T *et al*. Evaluation of general 16S ribosomal RNA gene PCR primers for classical and next-generation sequencing-based diversity studies. *Nucleic Acids Res* 2013;**41**:e1–e.

Kraft B, Tegetmeyer HE, Sharma R *et al*. The environmental controls that govern the end product of bacterial nitrate respiration. *Science* 2014;**345**:676–9.

Kumar S, Herrmann M, Blohm A *et al*. Thiosulfate- and hydrogen-driven autotrophic denitrification by a microbial consortium enriched from groundwater of an oligotrophic limestone aquifer. *FEMS Microbiol Ecol* 2018a;**94**:fiy141.

Kumar S, Stecher G, Li M *et al*. MEGA X: molecular evolutionary genetics analysis across computing platforms. *Mol Biol Evol* 2018b;**35**:1547–9.

Lee PA, Tullman-Ercek D, Georgiou G. The bacterial twin-arginine translocation pathway. *Annu Rev Microbiol* 2006;**60**:373–95.

Liu B, Mao Y, Bergaust L *et al*. Strains in the genus Thauera exhibit remarkably different denitrification regulatory phenotypes. *Environ Microbiol* 2013;**15**:2816–28.

Lueders T, Manefield M, Friedrich MW. Enhanced sensitivity of DNA- and rRNA-based stable isotope probing by fractionation and quantitative analysis of isopycnic centrifugation gradients. *Environ Microbiol* 2004;**6**:73–8.

Lycus P, Lovise Bøthun K, Bergaust L *et al*. Phenotypic and genotypic richness of denitrifiers revealed by a novel isolation strategy. *ISME J* 2017;**11**:2219–32.

Mair P, Wilcox R. Robust statistical methods in R using the WRS2 package. *Behav Res Methods* 2019, DOI: 10.3758/s13428-019-01246-w.

McMurdie PJ, Holmes S. phyloseq: an R package for reproducible interactive analysis and graphics of microbiome census data. *PLoS One* 2013;**8**. DOI: 10.1371/journal.pone.0061217.

Mosier AR. Soil processes and global change. *Biol Fertil Soils* 1998;**27**:221–9.

Nozawa-Inoue M, Jien M, Yang K *et al*. Effect of nitrate, acetate, and hydrogen on native perchlorate-reducing microbial communities and their activity in vadose soil. *FEMS Microbiol Ecol* 2011;**76**:278–88.

Oksanen J, Blanchet FG, Friendly M *et al*. vegan: community ecology package. 2019, https://CRAN.R-project.org/package=vegan (03 February 2020, date last accessed).

Oren A. The family Rhodocyclaceae. In: Rosenberg E, DeLong EF, Lory S, Stackebrandt E, Thompson F (eds.) *The Prokaryotes: Alphaproteobacteria and Betaproteobacteria*, Berlin Heidelberg: Springer, 2014, 975–98.

Quast C, Pruesse E, Yilmaz P *et al*. The SILVA ribosomal RNA gene database project: improved data processing and web-based tools. *Nucleic Acids Res* 2012;**41**:D590–D6.

R Development Core Team. R: a language and environment for statistical computing. *R Foundation for Statistical Computing*, 2019.

Richardson DJ, Berks BC, Russell DA *et al*. Functional, biochemical and genetic diversity of prokaryotic nitrate reductases. *Cell Mol Life Sci CMLS* 2001;**58**:165–78.

Rivett MO, Buss SR, Morgan P *et al*. Nitrate attenuation in groundwater: a review of biogeochemical controlling processes. *Water Res* 2008;**42**:4215–32.

Salinero KK, Keller K, Feil WS *et al*. Metabolic analysis of the soil microbe *Dechloromonas aromatica* str. RCB: indications of a surprisingly complex life-style and cryptic anaerobic pathways for aromatic degradation. *BMC Genomics* 2009;**10**:351.

Salter SJ, Cox MJ, Turek EM *et al*. Reagent and laboratory contamination can critically impact sequence-based microbiome analyses. *BMC Biol* 2014;**12**:87.

Schnobrich MR, Chaplin BP, Semmens MJ *et al*. Stimulating hydrogenotrophic denitrification in simulated groundwater containing high dissolved oxygen and nitrate concentrations. *Water Res* 2007;**41**:1869–76.

Schullehner J, Hansen B, Thygesen M *et al*. Nitrate in drinking water and colorectal cancer risk: a nationwide population-based cohort study. *Int J Cancer* 2018. DOI: 10.1002/ijc.31306. Epub 2018 Feb 23.

Smith RL, Miller DN, Brooks MH *et al*. In situ stimulation of groundwater denitrification with formate to remediate nitrate contamination. *Environ Sci Technol* 2001;**35**:196–203.

Szekeres S, Kiss I, Kalman M *et al*. Microbial population in a hydrogen-dependent denitrification reactor. *Water Res* 2002;**36**:4088–94.

Töwe S, Albert A, Kleineidam K *et al.* Abundance of microbes involved in nitrogen transformation in the rhizosphere of *Leucanthemopsis alpina* (L.) Heywood grown in soils from different sites of the Damma Glacier Forefield. *Microb Ecol* 2010;**60**:762–70.

Töwe S, Wallisch S, Bannert A *et al.* Improved protocol for the simultaneous extraction and column-based separation of DNA and RNA from different soils. *J Microbiol Methods* 2011;**84**:406–12.

Vasiliadou IA, Pavlou S, Vayenas DV. A kinetic study of hydrogenotrophic denitrification. *Process Biochem* 2006a;**41**:1401–8.

Vasiliadou IA, Siozios S, Papadas IT *et al.* Kinetics of pure cultures of hydrogen-oxidizing denitrifying bacteria and modeling of the interactions among them in mixed cultures. *Biotechnol Bioeng* 2006b;**95**:513–25.

Wang O, Melnyk RA, Mehta-Kolte MG *et al.* Functional redundancy in perchlorate and nitrate electron transport chains and rewiring respiratory pathways to alter terminal electron acceptor preference. *Front Microbiol* 2018; **9**:376.

Wang Z, Li W, Li H *et al.* Phylogenomics of rhodocyclales and its distribution in wastewater treatment systems. *Sci Rep* 2020;**10**:3883.

Ward MH, Jones RR, Brender JD *et al.* Drinking water nitrate and human health: an updated review. *Int J Environ Res Public Health* 2018;**15**:1557.

Wild L, Mayer B, Einsiedl F. Decadal delays in groundwater recovery from nitrate contamination caused by low O2 reduction rates. *Water Resour Res* 2018;**54**: 9996–10012.

Yoon S, Nissen S, Park D *et al.* Nitrous oxide reduction kinetics distinguish bacteria harboring Clade I NosZ from those harboring Clade II NosZ. *Appl Environ Microbiol* 2016;**82**:3793–800.

Zhang Y, Zhong F, Xia S *et al.* Autohydrogenotrophic denitrification of drinking water using a polyvinyl chloride hollow fiber membrane biofilm reactor. *J Hazard Mater* 2009;**170**:203–9.

Zhao HP, Van Ginkel S, Tang Y *et al.* Interactions between perchlorate and nitrate reductions in the biofilm of a hydrogen-based membrane biofilm reactor. *Environ Sci Technol* 2011;**45**:10155–62.

Zumft WG. Cell biology and molecular basis of denitrification. *Microbiol Mol Biol Rev* 1997;**61**:533–616.